

# Dual-Octave-Bandwidth RF-Input Pseudo-Doherty Load Modulated Balanced Amplifier with $\geq 10$ -dB Power Back-off Range

Yuchen Cao and Kenle Chen

INSPIRE Lab, University of Central Florida, USA

yuchencao@knights.ucf.edu, kenle.chen@ucf.edu

**Abstract**— This paper presents the first-ever dual-octave bandwidth Pseudo-Doherty load-modulated balanced amplifier (PD-LMBA), well-suited for emerging 4G/5G communications and multi-band operations. This design is based on a special bias setting of balanced amplifier (peaking) and control amplifier (carrier), which are combined with proper amplitude and phase controls. The optimal load modulation (LM) of the balanced amplifier can be achieved together with reduced LM factor of the carrier amplifier, leading to maximized overall efficiency throughout extended output power back-off (OBO). With de-coupled cooperation of BA and CA, this architecture fundamentally breaks the bandwidth limitation imposed on load-modulated PAs. To demonstrate the principle, a ultra-wideband RF-input LMBA has been developed using GaN technology from 0.55–2.2 GHz. The experimental results exhibit an efficiency of 49–82% for peak output power and 40–64% for 10-dB OBO, respectively.

**Keywords**— Load modulation, balanced amplifier, Doherty, power amplifier, high efficiency, wideband, high-PAPR.

## I. INTRODUCTION

The booming of the 5G communications ecosystems and the maturity of technology have triggered the ever-increasing demands for high data rate, low latency, and high capacity of wireless connectivity. This requires complexly modulated radio waves, such as orthogonal frequency division multiplexing (OFDM), leading to large amplitude fluctuations quantified as high peak-to-average power ratio (PAPR). On the other hand, due to the highly scattered wireless spectrum allocation across the globe, a large number of PAs are required to cover the ultra-wide span of spectrum in order to support multi-band operation of wireless systems and global roaming.

To efficiently transmit high-PAPR signals, load modulation (LM) PAs have been identified as an effective solution. Among various load modulation techniques, Doherty power amplifier (DPA) is currently widely deployed in 4G systems (e.g., base stations) as a representative implementation of load modulation PA [1][2]. However, towards the applications to 5G systems, traditional DPAs face major challenges, including 1) limited output power back-off (OBO) range insufficient for emerging 4G/5G signals, 2) narrow bandwidth due to the quarter-wave inverter in its generic circuit topology. The recently proposed load modulation balanced amplifier (LMBA) [3][4] holds promising potential to extend both bandwidth and OBO range. With an additional signal injected into the isolation port of the balanced amplifier (BA)'s output quadrature coupler, the load impedance of BA can be modulated through changing the control signal's amplitude and phase. In addition, LMBA does not rely on the quarter-wave inverters, exhibiting promising

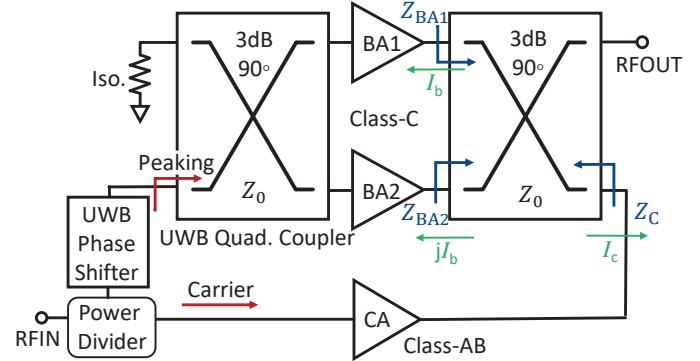


Fig. 1. General circuit schematic of the proposed ultra-wideband Pseudo-Doherty LMBA.

wideband potential. However, the power back-off range of reported LMBA designs is still not fully expanded beyond 6 dB, while the back-off efficiency optimization relies on concurrent amplitude and phase controls leading to difficulties in broadband design.

To fundamentally break the efficiency-bandwidth deadlock, this paper proposes a unique Doherty-like LMBA mode different from any existing LMBA and DPAs, which named Pseudo-Doherty LMBA (PD-LMBA). With special bias settings of BA and control amplifier (CA), as shown in Fig. 1, the CA's operation is independent to BA's impedance, leading to unlimited bandwidth in theory. Through properly designed phase and amplitude control, the LM of BA can be optimized to ensure maximum efficiency over the entire extended OBO range. Since no dynamic phase control is needed, a wideband phase shifter between BA and CA can be implemented using transmission line to result in RF-input design. The proposed theory and method are well validated by the developed PD-LMBA prototype, which experimentally demonstrates  $\geq 10$  of OBO and 120% of fractional bandwidth (the widest bandwidth to date).

## II. PSEUDO-DOHERTY LMBA

The RF-input LMBA described in Fig. 1 consists of a balanced amplifier and a control amplifier [5], the LM behavior of BAs is dependent on the power and phase of the control signal, which can be calculated as

$$Z_{BA1} = Z_{BA2} = Z_0 \left(1 + \frac{\sqrt{2}I_c e^{j\theta}}{I_b}\right). \quad (1)$$

where  $I_b$  is the magnitude of BA currents,  $I_c$  is the magnitude of CA current, and  $\theta$  is the phase of the control path.

### A. Pseudo-Doherty LMBA Theory

Different from the generic LMBA [3] and the reported Doherty-like LMBA [6], the balanced amplifiers in PD-LMBA are biased in Class-C acting as the ‘peaking amplifier’, while the CA is biased in Class-AB as the ‘carrier amplifier’, as depicted in Fig. 1. In theory, the operation of PD-LMBA can be mainly divided into the following two regions:

- **Low-Power Region ( $P_{\text{OUT}} < P_{\text{Max}}/\text{OBO}$ ):** In this region, the BAs are not turned on,  $I_b = 0$ . The impedances of BA1 and BA2 are thus equal to  $\infty$ , and the output power is completely generated by the CA, so that the overall LMBA efficiency is equal to the CA efficiency. The impedance of CA equal to  $Z_0$  calculated through Eqs. (1):

$$\begin{aligned} Z_{\text{BA1,LP}} &= Z_{\text{BA2,LP}} = \infty; \\ Z_{\text{C,LP}} &= Z_0. \end{aligned} \quad (2)$$

When the input power reaches the target OBO power, CA is designed to reach saturation for maximum back-off efficiency.

- **High-Power Region ( $P_{\text{Max}}/\text{OBO} \leq P_{\text{OUT}} \leq P_{\text{Max}}$ ):** As the power increases to the target OBO power, the BA is turned on and  $I_b$  starts to increase. Through the Eqs. (1) calculation, it is proved that the loading of CA remains to be  $Z_0$ , so that the saturation of CA can be maintained. As the power further increases to maximum, CA and BA are both saturated. Thus, the LM behavior of BA1, BA2 and the CA impedance are given by

$$\begin{aligned} Z_{\text{BA1,HP}} &= Z_{\text{BA2,HP}} = Z_0 \left( 1 + \frac{\sqrt{2} I_{c,\text{Max}} e^{j\theta}}{I_b} \right); \\ Z_{\text{C,HP}} &= Z_0. \end{aligned} \quad (3)$$

In this region, due to the LM controlled by CA, the efficiency of the BA can be significantly boosted, while the CA maintains the highest efficiency as saturated. As a result, the overall back-off efficiency of the PD-LMBA is optimized over the entire OBO.

### B. Amplitude and Phase Control

In order to obtain the maximum target power back-off efficiency under ideal conditions, CA needs to be saturated at target power which can be achieved by setting a suitable CA drain voltage. At the same time, BA needs to be turned on at target power to keep enhancing the overall efficiency of LMBA, which could be achieved by setting the power dividing ratio between BA and CA and properly choosing the depth of Class-C bias for BA [7].

It can be calculated from Eqs. (2) that the turn-on position of the BA load modulation is fixed on the Smith chart, and the LM trajectory is only determined by the phase of the CA input signal ( $\theta_{\text{ca}}$ ). It should be emphasized that this modulation method does not need to rely on dynamic phase modulation, which means any frequency has a fixed phase to optimize the carrier modulation trajectory to achieve the best back-off efficiency, as shown in Fig. 3(a).

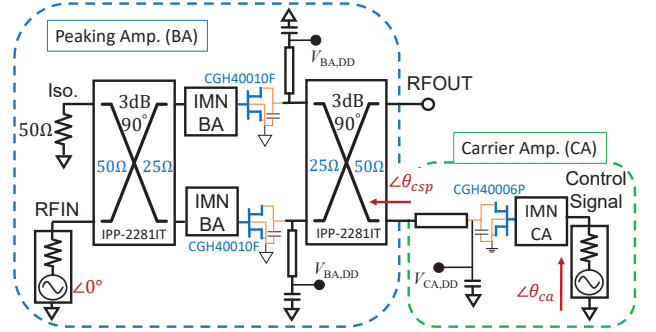


Fig. 2. Implementation of the proposed wideband PD-LMBA using wideband impedance-transformer coupler and GaN transistor (dual-input is for analysis only and will be merged to RF-input in the final design).

### C. Load Modulation of Carrier Amplifier

From theoretical calculation through Eqs. (2) (3),  $Z_C$  is consistently equal to  $Z_0$ . While this constant  $Z_C$  leads to a high CA efficiency during BA load modulation, it also causes over driving and potential clipping of CA. In actual conditions, moderate LM of CA can still be achieved. There are two main effects resulting in this carrier LM: 1) the device parasitics, which causes non- $\infty$  off-state impedance of BA; 2) the powers of BA1 and BA2 are not exactly equalized due to the non-ideal couplers. The resultant CA LM trajectory is also dependent on phase offset between BA and CA, which affects the CA efficiency throughout the entire OBO. In this design, the LM factor of carrier amplifier is reduced as compared to Doherty PA, in order to stabilize the  $Z_C$  trajectory after BAs are turned on, so that a high CA efficiency can be maintained. On the other hand, however, we can take advantage of carrier LM to mitigate the over-driving of CA and achieve better linearity.

## III. DESIGN OF ULTRA-WIDEBAND PD-LMBA

Following the PD-LMBA theory and the ideal schematic (Fig. 1), the physical circuits of the CA and BA in the ultra-wideband PD-LMBA are built using 6-W GaN transistor (Wolfspeed CGH40006P) and 10-W GaN transistors (Wolfspeed CGH40010F), respectively. The realized circuit schematic is shown in Fig. 2. In order to accommodate the high PAPR of emerging 4G/5G signals, the target OBO is set to 10 dB, and the target frequency range is from 0.55 to 2.2 GHz.

### A. Wideband BA and CA Design

Two impedance-transformer (2 : 1) couplers (IPPA-2281IT, Innovative Power Products) are employed at the input and output of the BA, which offer ultra-wide bandwidth with reduced complexity of matching network design. The impedance matching at the output is achieved by a combination of the impedance-transformer coupler and bias lines. This direct connection between the transistor and the coupler effectively reduces the broadband phase dispersion induced by the matching network [3].

The saturation efficiency of CA directly affects the back-off efficiency of the PD-LMBA, which is optimized through wideband efficiency-oriented matching of CA. Meanwhile,

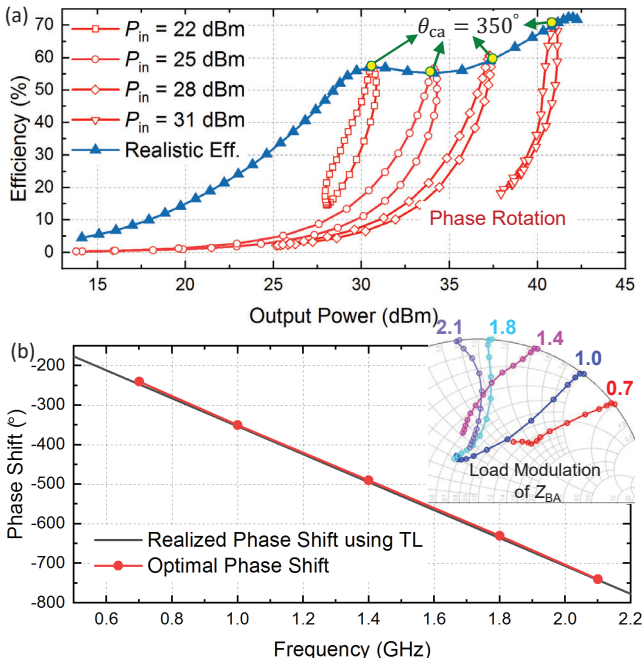


Fig. 3. (a) Determination of the optimal BA-CA phase offset based on dual-input circuit schematic in Fig. 2 at 1.0 GHz through phase-swept input stimulus of CA; (b) Determined optimal phase offset at different frequencies and realization using TL-based wideband phase shifter for merging the BA and CA inputs; (inset Smith chart) BA load-modulation trajectories with implemented phase shifter.



Fig. 4. Fabricated PD-LMBA prototype.

the load modulation ratio of CA is reduced. Therefore, the CA output matching is realized using a multi-segment transmission-line transformer. The input matching of CA and BA are designed using multi-stage low-pass matching network implemented with transmission lines [8].

#### B. Ultra-Wideband BA-CA Phase Shifter Design

The determination of optimal BA-CA phase offset is elaborated in Fig. 3(a). For any given frequency, there is a dedicated optimal phase offset resulting in the highest back-off efficiency. By extending this process over the entire bandwidth, the wideband phase offset target can be determined. It is interesting to note the optimal phase offset is almost linearly proportional to the frequency in a negative slope, as shown in Fig. 3(b). With this linear characteristic, a  $50\text{-}\Omega$  transmission line is added at the BA input to implement such a broadband phase shifter and provide accurate broadband phase control.

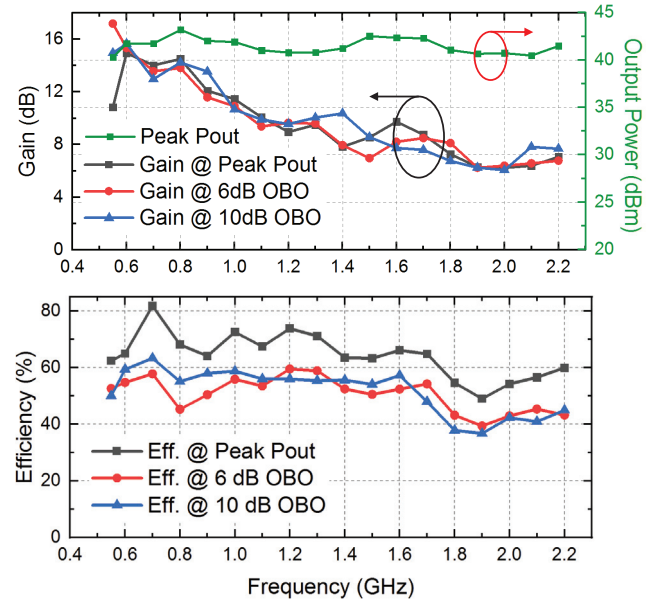


Fig. 5. Measured peak output power, gain and efficiency at various OBO levels from 0.55 to 2.2 GHz.

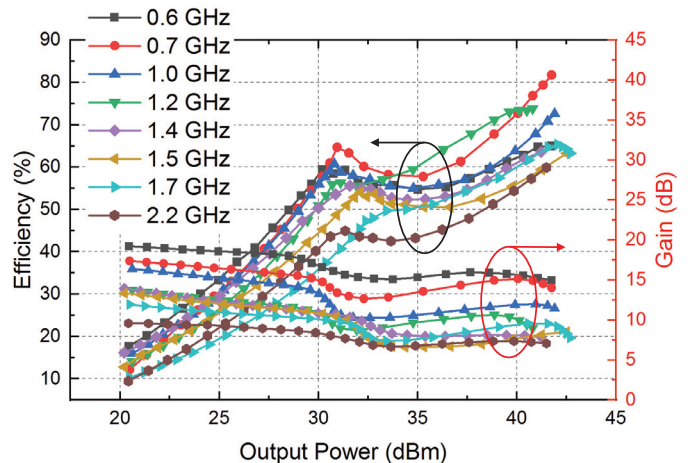


Fig. 6. Power-swept measurement of efficiency and gain from 0.6 to 2.2 GHz.

## IV. IMPLEMENTATION AND EXPERIMENTAL RESULTS

The PA is implemented on a 20-mil thick Rogers Duroid-5880 PCB board with a dielectric constant of 2.2. A photo of the fabricated PA is shown in Fig. 4. The CA is biased in Class-AB with a  $V_{DS,CA}$  around 12 V. The BA is biased in Class-C with 28-V  $V_{DS,BA}$ . A fine adjustment of bias voltages is performed at different frequencies to perfect the PA performance. The prototype is measured with both continuous-wave (CW) and modulated stimulation signals.

#### A. Continuous-Wave Measurement

In the continuous-wave measurement, a single-tone signal is used to measure the PD-LMBA performance from 0.55 to 2.2 GHz at different power levels. Fig. 5 shows the frequency response of the PD-LMBA. A peak output power of 41 – 43 dBm is measured across the entire bandwidth, together with

Table 1. State-of-the-Art of Wideband Load-Modulated Power Amplifiers

Ref. / Year	Architecture	Freq. (GHz)	FBW (%)	$P_{\text{Max}}$ (dBm)	DE @ $P_{\text{Max}}$ (%)	DE @ HBO (%)	DE @ LBO (%)
[9] 2018	DPA	1.5-3.8	86.8	42.3-43.4	42-63	33-55@6 dB	22-40@10 dB*
[10] 2018	3-Way DPA	0.6-0.9	40	46.1-46.9	51.1-78	51.9-66.2@6 dB	42-64@9.5 dB*
[11] 2019	3-Way DPA	1.6-2.6	48	45.5-46	53-66	52-66@6 dB	50-53@9.5 dB
[2] 2019	DEPA	2.55-3.8	40	48.8-49.8	54-67	42-53@6 dB*	47-60@8 dB
[12] 2018	Dual-Input LMBA	1.7-2.5	38	48-48.9	48-58*	43-53@6 dB*	33-45@10 dB*†
[5] 2017	RF-Input LMBA	1.8-3.8	71	44	46-70	33-59@6 dB	20-25@10 dB*†
This Work	PD-LMBA	0.55-2.2	120	41-43	49-82	40-60@6 dB	39-64@10 dB

\* Graphically estimated, † PAE.

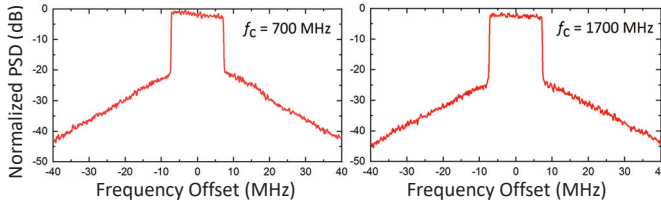


Fig. 7. Output spectrum from modulated measurement using a 10-MHz 9.5-dB-PAPR LTE signal centered at 700 and 1700 MHz.

8 – 15 dB gain at different OBO levels. The corresponding measured efficiency is 49 – 82%. The efficiencies at 6-dB and 10-dB OBOs are in the range of 40 – 60% and 39 – 64%, respectively. The power-dependent gain and efficiency profiles are shown in Fig. 6 at different frequencies. A strong Doherty-like efficiency-enhancement behavior is observed. In Table I, the performance of this design is compared to the best recently published wideband load-modulation PAs. It can be observed that the proposed PD-LMBA technology achieves high efficiency, large OBO range, and ultra-wide bandwidth that nearly doubles the state-of-the-art.

### B. Modulated Measurements

In order to validate the effectiveness of the PD-LMBA in realistic communications, a 10-MHz-bandwidth LTE signal with a PAPR of 9.5 dB is used to perform modulated testing. The modulated signals are generated and analyzed with Keysight PXIe vector transceiver (VXT M9421). For an average output power of 32 dBm, the measured output spectrum at 700 and 1700 MHz are shown in Fig. 7, with 62% and 51% average efficiency, respectively. The ACLR of the measured frequency are all higher than 24 dB without any digital predistortion.

### V. CONCLUSION

This paper introduces the design and implementation of Pseudo-Doherty LMBA, a new type of ultra wideband LMBA with extended OBO range. Based on a unique combination of CA and BA, this architecture results in decoupled co-operation of carrier and peaking amplifiers, thus fundamentally eliminating the bandwidth limitation imposed on classic active LM techniques. With proper phase and amplitude controls, an optimal LM behavior can be achieved for PD-LMBA leading to maximized efficiency over extended power back-off range. For any single frequency, the efficiency optimization can be achieved without dynamic phase tuning,

which greatly reduces the circuit complexity. The proposed technique is experimentally validated by a hardware prototype, demonstrating the capability of efficiently amplifying signals with 10 dB PAPR over 120% of fractional bandwidth. The performance of this technique has significantly advanced the state-of-the-art, exhibiting promising potential for applications in future multi-band wireless communication systems.

### REFERENCES

- [1] M. Özen, K. Andersson, and C. Fager, "Symmetrical Doherty power amplifier with extended efficiency range," *IEEE Transactions on Microwave Theory and Techniques*, vol. 64, no. 4, pp. 1273–1284, April 2016.
- [2] P. Saad, R. Hou, R. Hellberg, and B. Berglund, "An 80W power amplifier with 50% efficiency at 8db power back-off over 2.6-3.8 GHz," in *2019 IEEE MTT-S International Microwave Symposium (IMS)*, June 2019, pp. 1328–1330.
- [3] D. J. Sheppard, J. Powell, and S. C. Cripps, "An efficient broadband reconfigurable power amplifier using active load modulation," *IEEE Microwave and Wireless Components Letters*, vol. 26, no. 6, pp. 443–445, June 2016.
- [4] D. Collins, R. Quaglia, J. Powell, and S. Cripps, "Experimental characterization of a load modulated balanced amplifier with simplified input power splitter," in *2018 Asia-Pacific Microwave Conference (APMC)*, Nov 2018, pp. 461–463.
- [5] P. H. Pednekar, E. Berry, and T. W. Barton, "RF-input load modulated balanced amplifier with octave bandwidth," *IEEE Transactions on Microwave Theory and Techniques*, vol. 65, no. 12, pp. 5181–5191, Dec 2017.
- [6] P. H. Pednekar, W. Hallberg, C. Fager, and T. W. Barton, "Analysis and design of a Doherty-like RF-input load modulated balanced amplifier," *IEEE Transactions on Microwave Theory and Techniques*, vol. 66, no. 12, pp. 5322–5335, Dec 2018.
- [7] Y. Cao, H. Lyu, and K. Chen, "Load modulated balanced amplifier with reconfigurable phase control for extended dynamic range," in *2019 IEEE MTT-S International Microwave Symposium (IMS)*, June 2019, pp. 1335–1338.
- [8] K. Chen and D. Peroulis, "Design of highly efficient broadband class-E power amplifier using synthesized low-pass matching networks," *IEEE Transactions on Microwave Theory and Techniques*, vol. 59, no. 12, pp. 3162–3173, Dec 2011.
- [9] J. J. Moreno Rubio, V. Camarchia, M. Pirola, and R. Quaglia, "Design of an 87% fractional bandwidth Doherty power amplifier supported by a simplified bandwidth estimation method," *IEEE Transactions on Microwave Theory and Techniques*, vol. 66, no. 3, pp. 1319–1327, March 2018.
- [10] A. Barthwal, K. Rawat, and S. K. Koul, "A design strategy for bandwidth enhancement in three-stage Doherty power amplifier with extended dynamic range," *IEEE Trans. Microw. Theory Techn.*, vol. 66, no. 2, p. 1024–1033, Feb 2018.
- [11] J. Xia, W. Chen, F. Meng, C. Yu, and X. Zhu, "Improved three-stage Doherty amplifier design with impedance compensation in load combiner for broadband applications," *IEEE Transactions on Microwave Theory and Techniques*, vol. 67, no. 2, pp. 778–786, Feb 2019.
- [12] R. Quaglia and S. Cripps, "A load modulated balanced amplifier for telecom applications," *IEEE Transactions on Microwave Theory and Techniques*, vol. 66, no. 3, pp. 1328–1338, March 2018.